

# A STUDY ON BINARY COLLISION OF GNF DROPLETS USING A CONSERVATIVE LEVEL-SET METHOD

Ahmad Amani<sup>1</sup>, Nestor Balcázar<sup>2</sup>, Alireza Naseri<sup>3</sup> AND Asensi Oliva<sup>4</sup>

Heat and Mass Transfer Technological Center (CTTC)  
Universitat Politecnica de Catalunya - BarcelonaTech (UPC)  
ESEIAAT, C/ Colom 11, 08222 Terrassa (Barcelona), Spain  
web page: <http://www.cttc.upc.edu/>

<sup>1</sup>Ahmad@cttc.upc.edu

<sup>2</sup>nestor@cttc.upc.edu

<sup>3</sup>anaseri@cttc.upc.edu

<sup>4</sup>oliva@cttc.upc.edu

**Key words:** Numerical Simulation, Conservative Level-Set, Droplet Collision

**Abstract.** In this study, numerical simulations of binary droplet collisions of two GNF droplets are carried out. Navier-Stokes equations are solved for fluid motion both inside and outside of the droplet using a conservative level-set/finite-volume approach. On head-on collision of equal-sized droplets, implementation of symmetry boundary condition along with ghost nodes are used to mimic the behavior of the droplet colliding an image of itself while only one-eight of the domain being solved. A novel lamella stabilization approach is used which enables us to simulate extreme collision cases in relatively coarse meshes. The results are compared with available experimental and numerical results.

## 1 INTRODUCTION

The droplet collision phenomena is of relevance to many natural and industrial applications, including raindrop and cloud formation, spray coating, combustion and ink-jet printing. In many of these applications, the droplets exhibit non-Newtonian behavior. Droplet collision has been subject of numerous investigations, including experimental, analytical and numerical studies. The numerical simulation of multiphase flows is a challenging topic regarding the issues related to the tracking of interfaces, mass conservation of the droplet, and instabilities encountered by large density ratio and surface tensions.

Different experimental studies of the head-on and off-center collisions of droplets have been reported in literature. [1] studied the binary collision of the water droplets for different size ratios. They identified two different types of separating collisions, i.e. reflexive and stretching separations. [2] studied the collision of an ethanol droplet with a water droplet. [3] studied the transition between different collision outcomes. Despite the interesting break-throughs done in these works, the provided images lack the sufficient time resolution and information describing the nature of the collision.

Numerical simulations can provide significant details on the nature of collision which are difficult or impossible to capture experimentally. For example extracting the velocity and vorticity fields in numerical simulations are easily done while it requires expensive equipments in experimental studies. In addition, the flexibility of numerical simulations on implementing different fluid properties make them more interesting on studying the fluid flows. Different numerical approaches are used to study the nature of binary droplet collisions, including Lattice Boltzmann (LB), front tracking (FT), level-set (LS), smoothed particle hydrodynamic (SPH), and volume of fluid (VOF) methods [4, 5, 6, 7, 8].

In this paper, we study the possibility of a general framework on simulation of binary collision of GNF droplets using a finite-volume discretization of conservative level-set method as introduced by [9]. The rest of the present paper is organized as follow: The mathematical formulation is presented in Section 2 . Numerical methods are described in Section 3. Model validation and numerical experiments are presented in Section 4 . Finally, concluding remarks are discussed in Section 5.

## 2 MATHEMATICAL FORMULATION

Navier-Stokes equations are used to describe the conservation of mass and momentum of two incompressible immiscible GNF fluids on a spacial domain of  $\Omega$  with boundary of  $\partial\Omega$ . These governing equations are as following [9]:

$$\begin{aligned} \frac{\partial}{\partial t}(\rho\mathbf{v}) + \nabla \cdot (\rho\mathbf{v}\mathbf{v}) &= -\nabla p + \nabla \cdot [\mu(\dot{\gamma}) (\nabla\mathbf{v} + (\nabla\mathbf{v})^T)] + \rho\mathbf{g} + \sigma\kappa\mathbf{n}\delta_{\Gamma} \text{ in } \Omega & (1) \\ \nabla \cdot \mathbf{v} &= 0 \text{ in } \Omega & (2) \end{aligned}$$

where  $\rho$  is density of the fluids,  $\mathbf{v}$  is the velocity field,  $p$  pressure field,  $\mathbf{g}$  gravitational acceleration and  $\delta_{\Gamma}$  is the Dirac delta function concentrated at the interface ( $\Gamma$ ). Also  $\mathbf{n}$  is the unit normal vector outward to interface,  $\kappa$  is the interface curvature,  $\sigma$  is the interface tension coefficient and  $\mu(\dot{\gamma})$  is the dynamic viscosity of the GNF fluid. For Newtonian fluids,  $\mu(\dot{\gamma}) = \mu$  is used and for non-Newtonian shear-thinning fluids a Carreau-Yasuda model is used as below:

$$\mu(\dot{\gamma}) = \mu_{\infty} + (\mu_0 - \mu_{\infty}) (1 + (\lambda\dot{\gamma})^a)^{(n-1)/a} \quad (3)$$

Where  $\mu_0$  and  $\mu_{\infty}$  are dynamic viscosity at zero and infinite shear rates, respectively,  $n$  is a power-law index, and  $a=0.557$  is a parameter which controls the transition between zero shear rate and the power-law regime [10]. In this formulation  $\lambda$  is a time constant calculated as follows:

$$\lambda = 250\pi\sqrt{\frac{\rho D^3}{8\sigma}} \quad (4)$$

Mass, density and viscosity can be defined as scalar-fields inside the whole domain as follows:

$$\rho = \rho_1 H + \rho_2 (1 - H) \quad (5)$$

$$\mu = \mu_1 H + \mu_2 (1 - H) \quad (6)$$

where  $H$  is the Heaviside step function which takes the value one in dispersed phase and zero elsewhere. The  $\mu_1$  and  $\mu_2$  values in each phase are calculated based on the related GNF model. In this research conservative level-set (CLS) method [11], as introduced by Balcázar et. al. [9] is used. Conservative LS method employs a regularized indicator function  $\phi$  as below:

$$\phi(x, t) = \frac{1}{2} \left( \tanh \left( \frac{d(x, t)}{2\varepsilon} \right) + 1 \right) \quad (7)$$

where  $\varepsilon$  is the parameter that sets the thickness of the interface.  $\phi$  varies from 0 in one fluid to 1 in other fluid. velocity vector field,  $\mathbf{v}$ , provided from solution of Navier-Stokes equations is used to advect the level-set function [9, 11]:

$$\frac{\partial \phi}{\partial t} + \nabla \cdot \phi \mathbf{v} = 0 \quad (8)$$

In order to keep the profile and thickness of the interface constant, an additional re-initialization equation [12] is used:

$$\frac{\partial \phi}{\partial \tau} + \nabla \cdot \phi (1 - \phi) \mathbf{n}_{\tau=0} = \nabla \cdot \varepsilon \nabla \phi \quad (9)$$

which is advanced in pseudo-time  $\tau$ . Normal vector  $\mathbf{n}$  on the interface and curvature  $k$  of the interface, are obtained using [9]:

$$\mathbf{n} = \frac{\nabla \phi}{\|\nabla \phi\|} \quad (10)$$

$$k(\phi) = -\nabla \cdot \mathbf{n} \quad (11)$$

The continuous surface force model (CSF) [13] is used for surface tension computation which converts the term  $\sigma \kappa \mathbf{n} \delta_\Gamma$  in Eq. 1 to a volume force term as follows:

$$\sigma \kappa \mathbf{n} \delta_\Gamma = \sigma \kappa(\phi) \nabla \phi \quad (12)$$

### 3 NUMERICAL METHOD

Finite-volume (FV) approach is used to discretize the Navier-Stokes and level-set equations. collocated grid arrangement is used in discretization of the domain where all the computed variables are stored at cell centers [9].

A central difference (CD) scheme is used to discretize the diffusion term of the momentum and compressive term of re-initialization equation (9). A distance-weighted linear interpolation is used to calculate the face values of physical properties and interface normals. The gradients are computed at the cell centroids using the least-squares method. In order to improve the numerical stability of the solver, a total-variation Diminishing (TVD) SUPERBEE flux limiter is used to discretize the convective term as implemented in [9]. A classical fractional step projection method as described by [14] is used to solve the velocity-pressure coupling. The solution procedure is as follows:

- Physical properties, interface geometric properties and velocity field are initialized.
- Allowable time step limited by CFL conditions is calculated.
- The advection equation (8) is integrated in time with a 3-step third order accurate TVD Runge-Kutta scheme [15].
- The re-initialization equation (9) is integrated in pseudo time ( $\tau$ ) using a third order accurate TVD Runge-Kutta scheme. One iteration is used to solve the discretized form of this equation.
- Physical properties in the domain (density and viscosity) and geometrical properties at the interface (curvature and interface normal) are updated from the level-set and shear fields.
- The velocity and pressure fields are calculated using fractional-step method. In this formulation, the first step is to calculate the predicted velocity  $\mathbf{v}$ . Fully explicit second-order Adam-Bashforth method is used to discretize the prediction step:

$$\frac{\rho \mathbf{v}^* - \rho^n \mathbf{v}^n}{\Delta t} = \frac{3}{2}(R_v^v)^n - \frac{1}{2}(R_v^v)^{n-1} \quad (13)$$

where  $R_v^v = -\mathbf{C}_h(\rho \mathbf{v}) + \mathbf{D}_h(\mathbf{v}) + \rho \mathbf{g} + \sigma \kappa \nabla_h(\phi)$ . In this equation  $\mathbf{C}_h(\rho \mathbf{v}) = \nabla_h \cdot (\rho \mathbf{v} \mathbf{v})$  is the convective operator,  $\mathbf{D}_h(\mathbf{v}) = \nabla_h \cdot [\mu(\dot{\gamma})(\nabla_h \mathbf{v} + \nabla_h^T \mathbf{v})]$  is the diffusion operator and  $\nabla_h$  is the gradient operator. In the next step, pressure field is calculated by solving the Poisson equation:

$$\nabla_h \cdot \left( \frac{1}{\rho} \nabla_h(p^{n+1}) \right) = \frac{1}{\Delta t} \nabla_h \cdot (\mathbf{v}^*) \quad (14)$$

The resulting velocity  $\mathbf{v}^*$  does not satisfy the continuity equation and needs to be corrected by:

$$\mathbf{v}^{n+1} = \mathbf{v}^* - \frac{\Delta t}{\rho} \nabla_h(p^{n+1}) \quad (15)$$

- repeat to reach the desired time.

The numerical methods are implemented in an in-house parallel c++/MPI code called TermoFluids [16]. Validations and verifications of the numerical methods used in this work are reported in [9, 17, 12, 18, 19, 20].

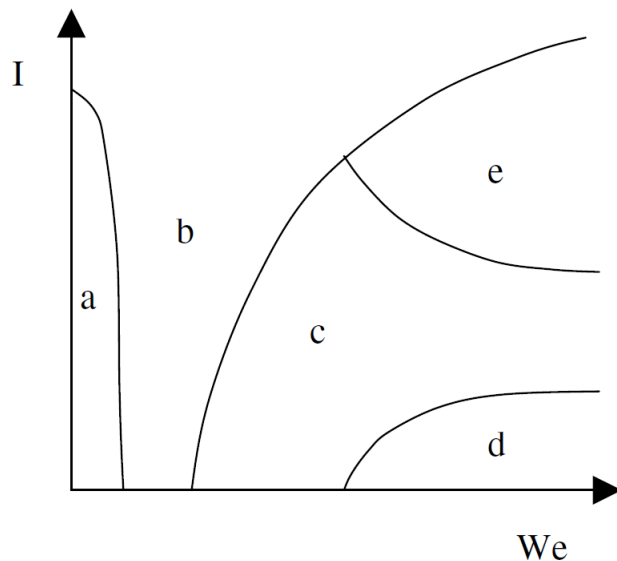


Figure 1: We-I diagram for collision outcome regimes

#### 4 RESULTS AND DISCUSSION

Experimental droplet collision studies are providing us with different correlations to understand what is the outcome of droplets collision. The main parameters are the surface tension coefficient  $\sigma$ , liquid viscosity  $\mu_l$ , liquid density  $\rho_l$ , droplets relative velocity  $U_{rel}$ , and the impact parameter  $I$ . The following non-dimensional parameters are thus defined by most authors to characterize the droplet's collision:

$$We = \frac{\rho_d U_{rel}^2 D}{\sigma}, \quad Re = \frac{\rho_d U_{rel} D}{\mu_l}, \quad Oh = \frac{\mu_d}{\sqrt{\rho_d \sigma D}}, \quad I = \frac{b}{D} \quad (16)$$

where  $We$  is the Weber number,  $Oh$  is the Ohnesorge number,  $D$  is the droplet diameter. Note that  $d$  stands for the droplet. The impact parameter  $I$  characterizes the eccentricity of the collision with  $b$  the inter-center distance of droplets. Collision regimes usually classifies in five main regimes as depicted in We-I diagram of figure 1:

- a. coalescence after minor deformation
- b. bouncing
- c. coalescence after substantial deformation
- d. coalescence followed by separation for near head-on collisions (Reflexive separation)
- e. coalescence followed by separation for off-center collisions (Stretching Separation)

During the collision process, a thin gas film is formed between the droplets. The consistency of this gas film during the collision process results in bouncing and rupture of it results in coalescence of the droplets. The thickness of this gas film is in the order of nanometers. Numerical resolution of this gas film requires numerical simulations in molecular levels such as Molecular Dynamics (MD) techniques and CFD simulation of

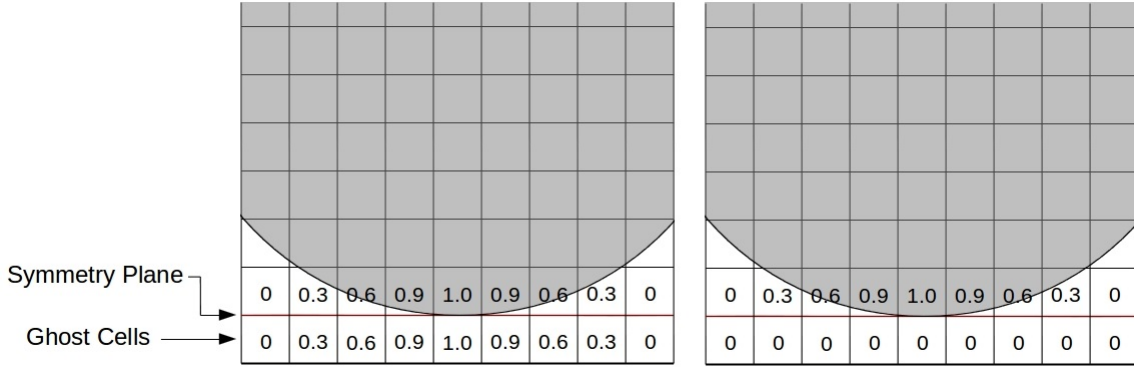


**Figure 2:** Illustration of the implemented ghost nodes and symmetry plane, along with two possible implementations of level-set boundary condition in ghost nodes. Left: Neumann BC. Right: Dirichlet BC.

it is almost impossible. In this study we have used ghost nodes to control the gas film rupture for cases of regimes a, b and c. For these cases, instead of collision of two droplets, collision of a droplet to a symmetry wall with ghost nodes is studied. Figure 2 illustrates the concept of ghost nodes in determining the droplet collision outcome. Implementing the Neumann boundary condition for level-set function in the ghost nodes, imitates the rupture of the gas film, resulting in coalescence of the droplets. On the other hand, Implementing the Dirichlet boundary condition for level-set function in these nodes imitates the persistence of gas film and thus bouncing of droplets. Changing the boundary condition of level-set function in these ghost nodes from Dirichlet to Neumann in a prescribed time enables us to model the retarded coalescence phenomenas (coalescence after minor deformation in regime "a" and coalescence after substantial deformation of moderate cases in regime "c").

Similar to the work of [21], to determine the rupture time of the gas film, a pre-simulation must be done. In this simulation, Dirichlet boundary condition for level-set function in ghost nodes is applied to model the persistence of gas film. The thickness of the gas film is being monitored throughout the whole simulation. The time in which this parameter reaches its minimum thickness is counted as rupture time of the gas film. In the next step, the simulation is being restarted. For times before calculated rupture time, Dirichlet boundary condition and for times after that, Neumann boundary condition on level-set function in ghost nodes are being applied. Rupture time for case "a" is calculated as explained and is  $t_{rupture}/t^* = 0.7682$ , where  $t_{rupture}$  is rupture time since the moment that two droplets collide and  $t^* = D/U_{rel}$  is used to non-dimensionalize it. Gas film rupture time of  $\infty$  means bouncing and 0.0 means immediate coalescence. The characteristics of the simulations of this study are presented in table 1. The Density and viscosity ratios for all the simulations are  $\rho_d/\rho_m = 666$  and  $\mu_d/\mu_m = 120$ , respectively, where m stands for matrix. A grid size of  $h=d/30$  is used in all the simulations. The collision happens in X direction. Symmetry boundary condition is applied when possible to reduce the computational costs.

Figures 3, 4 and 5 present the snapshots of the outcome of the droplets collision for cases

**Table 1:** Characteristics of the simulations

Case	We	Re	I	$L_x/D \times L_y/D \times L_z/D$	$t_{rupture}/t^*$
a	2.25	46.6	0	$2.5 \times 1.5 \times 1.5$	0.7682
b	2.27	59.0	0	$2.5 \times 1.5 \times 1.5$	$\infty$
d	61.4	296.5	0.06	$5.0 \times 2.8 \times 1.4$	0.0
nm	40.	8.0	0.0	$5.0 \times 2.8 \times 2.8$	0.0

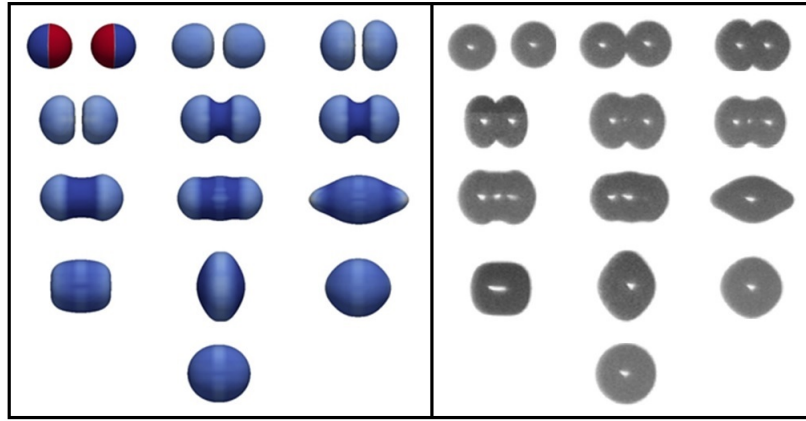


**Figure 3:** Retarded coalescence of droplets with minor deformation. Collision properties as of case 'a' in table 1. Left: results of current study, with velocity magnitude contours, right: experimental results of [22].

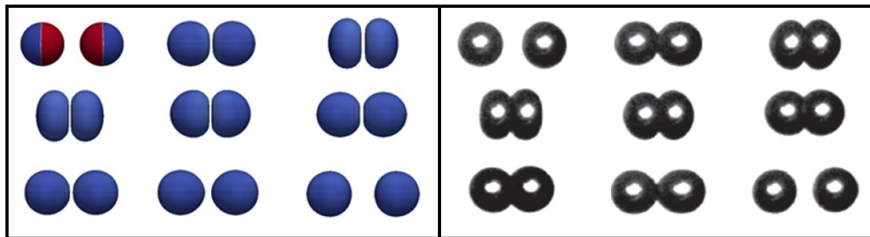


**Figure 4:** Bouncing of droplets with collision properties of case 'b' in table 1. Left: results of current study, with velocity magnitude contours, right: experimental results of [22].

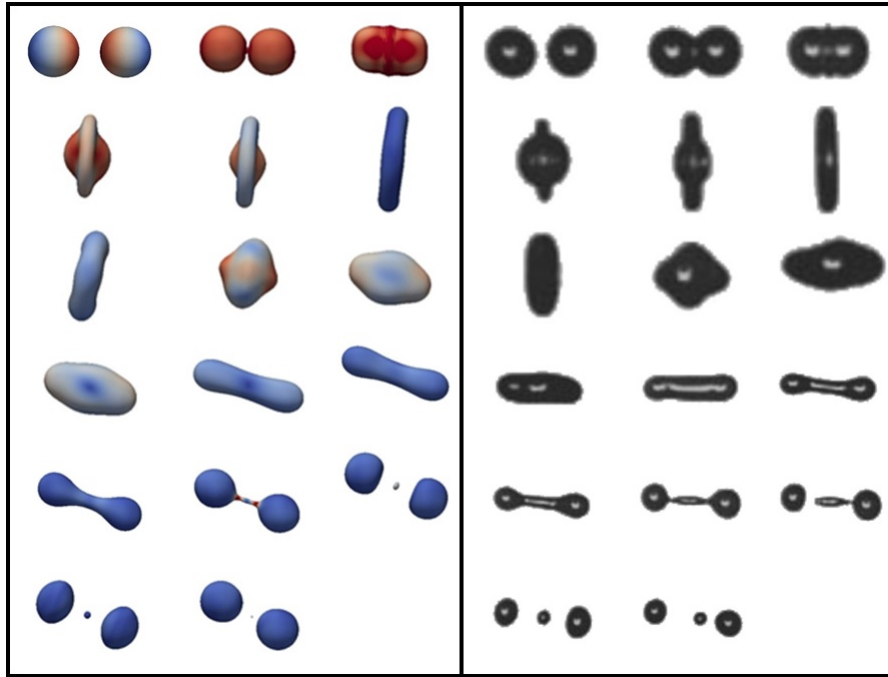


**Figure 5:** Immediate coalescence followed by reflexive separation. Collision properties as of case 'd' in table 1. Left: results of current study, with pressure contours on droplet surface, right: experimental results of [3].

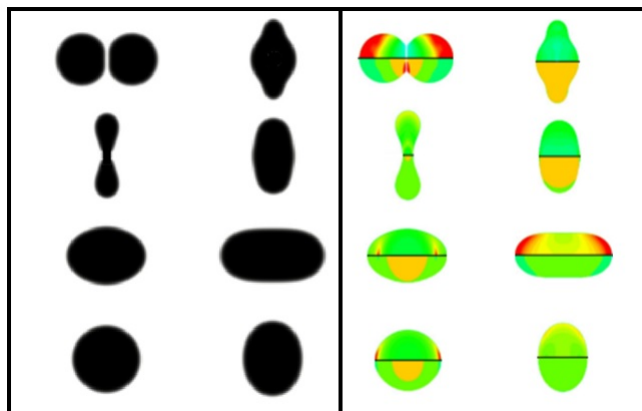


**Figure 6:** Immediate coalescence of collision of non-Newtonian shear-thinning droplets with  $n = 0.7$ ,  $Oh_0 = 0.795$  and  $Oh_\infty = 0.0265$ . Properties as of case 'nn' in table 1. Left: results of current study, right: numerical results of [23].

a, b and d, respectively. These figures are being compared with the available experimental results in the literature. The snapshots are made in the same time instances as the experimental figures. A new lamella stabilization approach is used to numerically stabilize the thin lamella film in case d. Figure 6 illustrates the results of collision of two shear-thinning non-Newtonian droplets compared with available numerical results of [23] in the same time instances. Good agreement is seen in all the cases.

## 5 CONCLUSION

In this paper, we present a numerical method to simulate collision of GNF droplets. The bouncing and retarded coalescence of the droplets can be controlled through the proper boundary condition in the ghost nodes. The gas film rupture time of retarded coalescence cases can be extracted through analysis of the gas film thickness. A lamella stabilization approach can be used to stabilize the lamella thin film and prevent it from rupturing numerically. During the whole simulations, the mass conservation of the droplets was satisfied. Results agree well with the references.

## Acknowledgments

This work has been financially supported by the *Ministerio de Economía y Competitividad, Secretaría de Estado de Investigación, Desarrollo e Innovación*, Spain (ENE2015-70672-P), and a FI research scholarship by the *Agència de Gestió d'Ajuts Universitaris i de Recerca (AGAUR)* of Generalitat de Catalunya.

## REFERENCES

- [1] N. Ashgriz and J. Y. Poo, “Coalescence and separation in binary collisions of liquid drops,” *Journal of Fluid Mechanics*, vol. 221, pp. 183–204, 1990.
- [2] T.-C. Gao, R.-H. Chen, J.-Y. Pu, and T.-H. Lin, “Collision between an ethanol drop and a water drop,” *Experiments in Fluids*, vol. 38, pp. 731–738, 6 2005.
- [3] J. Qian and C. K. Law, “Regimes of coalescence and separation in droplet collision,” *Journal of Fluid Mechanics*, vol. 331, pp. 59–80, 1997.
- [4] A. Mazloomi Moqaddam, S. S. Chikatamarla, and I. V. Karlin, “Simulation of Droplets Collisions Using Two-Phase Entropic Lattice Boltzmann Method,” *Journal of Statistical Physics*, vol. 161, no. 6, pp. 1420–1433, 2015.
- [5] M. Kwakkel, W. P. Breugem, and B. J. Boersma, “Extension of a CLSVOF method for droplet-laden flows with a coalescence/breakup model,” *Journal of Computational Physics*, vol. 253, pp. 166–188, 2013.
- [6] X. Jiang and A. J. James, “Numerical simulation of the head-on collision of two equal-sized drops with van der Waals forces,” *Journal of Engineering Mathematics*, vol. 59, no. 1, pp. 99–121, 2007.

- [7] S. Tanguy and A. Berlemont, “Application of a level set method for simulation of droplet collisions,” *International Journal of Multiphase Flow*, vol. 31, pp. 1015–1035, 2005.
- [8] M. R. Nobari, Y.-J. Jan, and G. Tryggvason, “Head-on Collisions of Drops - A Numerical Investigation,” *Physics of Fluids*, vol. 8, no. 1, pp. 29–42, 1996.
- [9] N. Balcázar, L. Jofre, O. Lehmkuhl, J. Castro, and J. Rigola, “A finite-volume/level-set method for simulating two-phase flows on unstructured grids,” *International Journal of Multiphase Flow*, vol. 64, pp. 55–72, 2014.
- [10] M. P. Escudier, I. W. Gouldson, A. S. Pereira, F. T. Pinho, and R. J. Poole, “On the reproducibility of the rheology of shear-thinning liquids,” *Journal of Non-Newtonian Fluid Mechanics*, vol. 97, no. 2, pp. 99–124, 2001.
- [11] E. Olsson and G. Kreiss, “A conservative level set method for two phase flow,” *Journal of Computational Physics*, vol. 210, no. 1, pp. 225–246, 2005.
- [12] N. Balcázar, O. Lehmkuhl, J. Rigola, and A. Oliva, “A multiple marker level-set method for simulation of deformable fluid particles,” *International Journal of Multiphase Flow*, vol. 74, pp. 125–142, 2015.
- [13] J. U. Brackbill, D. B. Kothe, and C. Zemach, “A continuum method for modeling surface tension,” *Journal of Computational Physics*, vol. 100, no. 2, pp. 335–354, 1992.
- [14] A. J. Chorin, “Numerical solution of the Navier-Stokes equations,” *Mathematics of computation*, vol. 22, no. 104, pp. 745–762, 1968.
- [15] S. Gottlieb and C.-W. Shu, “Total variation diminishing Runge-Kutta schemes,” *Mathematics of computation of the American Mathematical Society*, vol. 67, no. 221, pp. 73–85, 1998.
- [16] “Termo Fluids S.L.” [\url{http://www.termofluids.com/}](http://www.termofluids.com/).
- [17] N. Balcázar, O. Lehmkuhl, L. Jofre, and A. Oliva, “Level-set simulations of buoyancy-driven motion of single and multiple bubbles,” *International Journal of Heat and Fluid Flow*, vol. 56, pp. 91–107, 2015.
- [18] N. Balcázar, O. Lehmkuhl, L. Jofre, J. Rigola, and A. Oliva, “A coupled volume-of-fluid/level-set method for simulation of two-phase flows on unstructured meshes,” *Computers and Fluids*, vol. 124, pp. 12–29, 2016.
- [19] N. Balcázar, J. Castro, J. Rigola, and A. Oliva, “DNS of the wall effect on the motion of bubble swarms,” *Procedia Computer Science*, vol. 108, no. Supplement C, pp. 2008–2017, 2017.

- [20] N. Balcázar, J. Rigola, J. Castro, and A. Oliva, “A level-set model for thermocapillary motion of deformable fluid particles,” *International Journal of Heat and Fluid Flow*, vol. 62, no. Part B, pp. 324–343, 2016.
- [21] X. Li and U. Fritsching, “Numerical investigation of binary droplet collisions in all relevant collision regimes,” *The Journal of Computational Multiphase Flows*, vol. 3, no. 4, pp. 207–224, 2011.
- [22] K. L. Pan, C. K. Law, and B. Zhou, “Experimental and mechanistic description of merging and bouncing in head-on binary droplet collision,” *Journal of Applied Physics*, vol. 103, no. 6, 2008.
- [23] K. Sun, P. Zhang, C. K. Law, and T. Wang, “Collision dynamics and internal mixing of droplets of non-Newtonian liquids,” *Physical Review Applied*, vol. 4, no. 5, pp. 1–11, 2015.